

The Effect of Organoclays on Thermomechanical Properties in Cross-linked Photopolymer Nanocomposites

Kwame Owusu-Adom, Department of Chemical & Biochemical Engineering, University of Iowa, Iowa City, IA, USA

Allan Guymon, Department of Chemical & Biochemical Engineering, University of Iowa, Iowa City, IA, USA

Introduction

Thiol-ene photopolymers composed of thiol monomers copolymerized with terminally unsaturated molecules (enes) are attracting renewed research and industrial interest due to their unique advantages over traditional (meth)acrylate systems.¹ Today, potential applications of thiol-ene photopolymers including biological systems, adhesives and coatings are being explored. Thiol-ene have many distinct advantages over traditional (meth)acrylate based polymers. The step-growth reaction mechanism allows delayed gelation, and reduced shrinkage.^{2,3} Unlike (meth)acrylate photopolymers, oxygen inhibition is reduced significantly or eliminated⁴ with rapid polymerizations rates. The reactions can also be initiated without addition of photoinitiators.⁴

Although thiol-ene photopolymers possess many desirable characteristics, current applications could be expanded by increasing their mechanical stability and glass transition temperatures. The flexibility of the thioether linkage in thiol-ene photopolymers imparts inadequate mechanical stability for many applications. To enhance thermal properties, mechanical stability and the range of mechanical properties available for material fabrication, incorporating inorganic nanoparticles into polymeric matrices currently have been of renewed interest because of increases in mechanical,^{5,6} thermal,^{6,7,8} optical⁹⁻¹¹ and electronic properties^{9,12,13} attained with relatively small concentrations of the nanoparticles. Clays are naturally occurring particles with nano-sized domains¹⁴ are intriguing candidates to form such nanocomposites. Clay nanocomposites using numerous polymeric hosts have recently been fabricated.^{5,6,15,16} Higher moduli, glass transition temperatures, heat distortion temperatures and gas barrier properties have been observed in thermally cured nanocomposites utilizing only low concentrations of clay. In photopolymerizable systems, it has been shown that higher thermo-mechanical properties are attainable in some matrices,¹⁷ and that incorporating polymerizable functionality onto the clay surfaces amplifies the extent of increase.¹⁸ To access the nano-scale aggregate sizes, the stack-like nature of clay particles need to be delaminated (exfoliated). In this regard, polymerizable clay nanoparticles and increasing monomer-clay chemical compatibility were utilized to induce higher degrees of exfoliation in difunctional acrylate systems.¹⁷ Although complete exfoliation was not obtained, acrylated organoclays dispersed in a tripropylene glycol diacrylate/trimethylolpropane tris(3-mercaptopropionate) formulation, higher Young's modulus, reduced shrinkage and faster photopolymerization rates were induced in the hybrid photopolymer nanocomposite.¹⁷

This study examines the influence of added organoclay on the thermo-mechanical properties of binary and ternary thiol-ene-methacrylate formulations. Specifically, changes in modulus of thiol-ene systems containing both polymerizable and non-polymerizable organoclay are investigated. Young's modulus and T_g measurements were investigated as a measure of mechanical and thermal properties

respectively. Studies are extended to ternary thiol-ene-methacrylate formulations in which the rigidity of the neat polymer is decreased. This was accomplished by blending different concentrations of multifunctional methacrylate monomer as well as changing the ene monomer to produce more rubbery networks. The impact of added organoclay on the mechanical and thermal properties of these samples is examined, and changes in their behavior explained in terms of reaction behavior and polymer network structure. Functional group conversion and cross-link density were examined to determine the impact of clay nanoparticles on the physical properties of thiol-ene photopolymers.

Experimental

Materials

Non-polymerizable organoclay, Cloisite 15A (CL15A, Southern Clay Products, Gonzalez, TX), was used in examining the impact of non-reactive organoclay on the physical properties of thiol-ene photopolymers. Tetradecyl-2-acryloyloxy(ethyl) dimethylammonium bromide (C14A), octadecyl-2-acryloyloxy(ethyl) dimethylammonium bromide (C18A), tetradecyl-2-acryloyloxy(ethyl) dimethylammonium bromide (C14MA) and undecylmethacryloyloxy trimethylammonium bromide (PM1) are quaternary ammonium surfactants used to generate (meth)acrylate functionalized organoclays for this study. The polymerizable organoclays were developed using Cloisite Na (Southern Clay Products, Gonzalez, TX), an unmodified clay mineral. 2,2-Bis[4-(2-ethoxy-3-methacryloxyprop-1-oxy)phenyl]-propane (EBGDMA, Sartomer, Exton, PA) was used as a homopolymerizable cross-linking agent. Pentaerythritol allyl ether (PEAE), 1,3,5-Triallyl-1,3,5-triazine-2,4,6(1*H*,3*H*,5*H*)-trione (TATATO) and pentaerythritol tetrakis(3-mercaptopropionate) (PETMP) were obtained from Sigma Aldrich. 2,2-dimethoxyphenyl acetophenone (DMPA, Ciba-Geigy) was the photoinitiator used. Except where noted, all samples contained 0.1 wt% DMPA and were used as received. Figure 1 shows chemical structures of monomers and surfactants used in this study.

Methods

Polymerizable organoclays were prepared as outlined elsewhere.¹⁹ Briefly, 10g of clay was dissolved in 1000ml of de-ionized water under continuous stirring. The mixture was sonicated for one hour. Requisite amount of surfactant based on desired extent of cation exchange was dissolved in a separate beaker. The clay mixture and surfactant solution were combined and stirred continuously for 12-24 hours. The slurry was centrifuged and washed several times to remove unbound surfactants in the organoclay. Viscoelastic properties were measured by either 3-point bending or dynamic mechanical analysis. Elastic/Young's moduli (E') were measured on rectangular samples with dimensions 2 mm x 2 mm x 10 mm using a hydraulic universal test system (858 Mini Bioix, MTS Systems Corporation, Eden Prairie, MN, USA) at a crosshead speed of 1 mm/min.²⁰ Glass transition temperature and rubbery modulus of samples were taken on rectangular samples (measuring 2 x 13 x 25 mm) in the tensile mode using a dynamic mechanical analysis (DMA-Q800, TA Instruments). Experiments were conducted using a temperature ramp of 3°C/min from -50°C – 100°C at a frequency of 1 Hz. Cross-link density was calculated at $T_g + 50^\circ\text{C}$ using Equation 1.²¹

$$v_e = \frac{E'}{3RT} \quad (1)$$

where v_e is the molar cross-link density, E' is tensile rubbery modulus, R is the ideal gas constant and T represents temperature at which E' was measured (typically $T_g + 50^\circ\text{C}$).

Photopolymerization kinetics was monitored utilizing real time infrared spectroscopy (RTIR, Nexus 670 IR). Approximately 25 μm thick samples were sandwiched between NaCl salt crystals and purged for 6 minutes prior to initiating photopolymerization. Thiol and methacrylate functional group conversions were monitored at 2575 cm^{-1} (S-H stretching) and 816 cm^{-1} (C=C out of plane bending) respectively.²² Allyl ether double bond conversion was monitored by following change in the peak height as a function of time for the stretching peak at 3080 cm^{-1} .²² Photo-rheometry studies were performed at low light intensities (0.8 mW/cm^2) to adequately capture the influence of organoclay on polymer shrinkage.

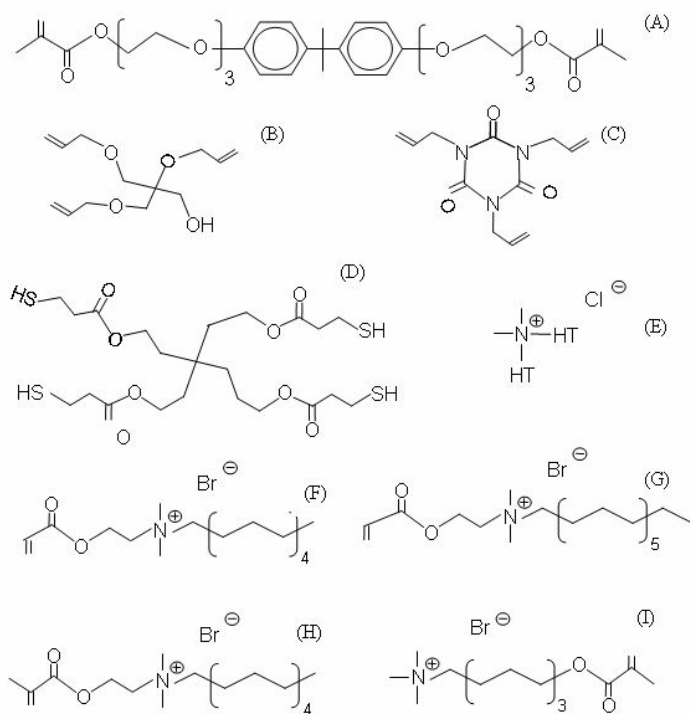


Figure 1. Chemical structures of (A) ethoxylated bisphenol (6A) dimethacrylate, EBGDMA, (B) pentaerythritol allyl ether, PEAE, (C) 1,3,5-Triallyl-1,3,5-triazine-2,4,6(1*H*,3*H*,5*H*)-trione, TATATO, (D) pentaerythritol tetrakis(3-mercaptopropionate), PETMP, (E) dimethyl dihydrogenated tallow, Me2HT, (F) tetradecyl-2-acryloyloxy(ethyl) dimethylammonium bromide, C14A, (G) octadecyl-2-acryloyloxy(ethyl) dimethylammonium bromide, C18A, (H) tetradecyl-2-acryloyloxy(ethyl) dimethylammonium bromide, C14MA, and (I) undecylmethacryloyloxy trimethylammonium bromide, PM1.

Results and Discussion

Previous studies incorporating clay nanoparticles into pure (meth)acrylate polymers produced nanocomposites with higher modulus, T_g and reduced shrinkage.¹⁸ To examine whether similar increases in the physical properties of thiol-ene polymers are observed, the elastic modulus of a 1:1 mol PETMP/TATATO mixture containing organoclay was examined utilizing a Hydraulic Universal Test System. Table 1 shows the elastic modulus of PETMP/TATATO samples that have 3 wt% or 5 wt% organoclay. Herein, acrylated organoclays (C14A or C18A-organoclay) rather than methacrylates were incorporated into the polymer matrix since the polymerization rates usually decreases significantly with addition of methacrylates to such thiol-ene polymerizations.²⁴ PETMP/TATATO photopolymers possess some of the highest modulus of any thiol-ene photopolymer system.⁹ Table 1 shows that adding 3 wt% Cloisite 15A to the pure polymer reduces the modulus by approximately 30%. As with behavior in (meth)acrylate polymers, addition of the polymerizable organoclay leads to increases in the elastic modulus relative to the Cloisite 15A system. However, the overall modulus decreases compared to the neat sample. Adding 3 wt% C14A-organoclay leads to the formation of a composite with approximately 25% lower elastic modulus in comparison to the neat system. With a relatively large-sized dispersant (C18A), the modulus reduces by less than 10% in comparison to the unfilled polymer. Elastic modulus

decreases further when the amount of organoclay is increased. With addition of 5 wt% Cloisite 15A, the modulus remains relatively unchanged from the 3 wt% system. On the other hand, the addition of polymerizable organoclay results in a significant reduction in elastic modulus. The C14A-organoclay sample has a modulus that is about 40% lower than the neat system, while greater than 60% decrease is observed with addition of similar concentrations of C18A-organoclay to the PETMP/TATATO polymer. The extent of functional group conversion upon adding 5 wt% C18A-organoclay to the thiol-ene mixture decreases substantially, and could help explain the lower modulus observed in the polymer samples.

Table 1. Elastic modulus of 1:1 molar mixture of PETMP and TATATO, measured at 25°C.

Monomer	Organoclay	Elastic Modulus (MPa)	
		3 wt% Organoclay	5 wt% Organoclay
PETMP/TATATO	None	983 ± 115	983 ± 115
	Cloisite 15A	668 ± 98	627 ± 90
	C14A-organoclay	731 ± 43	596 ± 111
	C18A-organoclay	891 ± 202	387 ± 61

To fabricate materials with a wider range of mechanical properties, ternary systems comprising (meth)acrylate and thiol-ene blends have been synthesized. Ethoxylated bisphenol dimethacrylate monomers have been incorporated into thiol-ene photopolymers to increase glass transition temperature and modulus.^{22,23} To examine if these mechanical properties could be changed further, EBGDMA-thiol-ene samples containing 3 wt% organoclay were examined via DMA. It has been shown previously that the ability of organoclay to elevate the modulus of nanocomposites increases in loosely cross-linked polymers. In addition, since thiol-ene photopolymers utilizing TATATO usually exhibits high rigidity, other elastomeric ene monomers for which addition of organoclays may better allow control of the

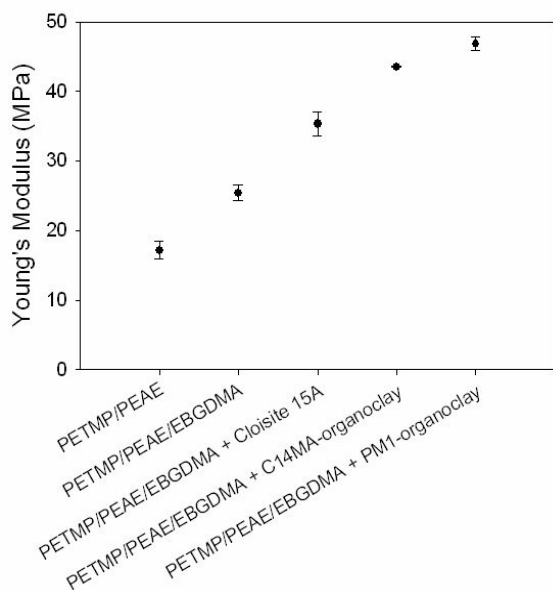


Figure 2. Young's modulus of 3 wt% organoclay in 70:30 wt% EBGDMA:PETMP/PEAE (1:1 mol PETMP:PEAE). DMA tests performed at 30°C using a 1 Hz frequency.

nanocomposite physical properties were investigated. Thiol-ene photopolymers in which the ene component is PEAE are rubbery at room temperature. Figure 2 shows the Young's modulus of ternary EBGDMA/PETMP/PEAE samples as a function of the type of organoclay. The samples were made of 70 wt% EBGDMA and 30 wt% PETMP/PEAE with equimolar functional group concentration of PETMP and PEAE.

The addition of EBGDMA to the thiol-ene mixture actually causes an increase in modulus for the neat ternary sample compared to the binary PETMP/PEAE formulation based on the different network structure as compared to the more rigid PETMP/TATATO system. Unlike the sample containing TATATO, EBGDMA induces greater modulus increases in the PETMP/PEAE mixture. In the more elastomeric EBGDMA/PETMP/PEAE system in which the modulus was decreased by adding EBGDMA (not shown), addition of just 3 wt% Cloisite 15A produces nanocomposites with slightly higher modulus than the unfilled polymer. The Young's modulus increases further

with addition of polymerizable organoclay, approaching nearly double the modulus of the neat samples. Approximately 40% higher modulus is observed when C14MA-organoclay is added to the polymer, while about 50% increase occurs with PM1-organoclay relative to the pristine polymer.

Dynamic mechanical analysis was also used to analyze changes induced in the polymer network as a result of incorporating organoclay into the matrix. By adding the thiol-ene monomers to EBGDMA, the T_g of the resulting polymer is reduced dramatically. A rubbery polymer is formed at room temperature, even with the relatively low molar concentration of the thiol-ene. The glass transition temperature reduces to approximately 22°C in the neat polymer system as shown in table 2. Little change is observed in the T_g with 3 wt% organoclay. Interestingly, while adding polymerizable organoclay nearly doubles the Young's modulus, the glass transition temperature remains unchanged. Samples with C14MA-organoclay actually exhibit slight decreases (*ca.* 3°C) relative to the unfilled polymer. Composites of both CL15A and PM1-organoclay, on the other hand, have approximately the same T_g as the neat polymer.

The changes in T_g differ from the behavior observed in previous studies of elastomeric PEGDA nanocomposites, in which addition of similar levels of organoclay concentrations resulted in elevated T_g even for samples that contained a non-polymerizable organoclay. To understand the evolution of the mechanical and thermal properties further, the reaction behavior and network structure was examined. Here, the focus was on the copolymerization behavior of the species to gain insights into potential changes to the network structure in relation to the more rigid samples containing TATATO. Examination of the polymer cross-link density (see Table 2) shows that similar cross-link densities are found in both the neat polymer and the CL15A nanocomposite. With C14MA-organoclay or PM1-organoclay, the cross-link density increases substantially. In the C14MA-organoclay nanocomposite, a 50% increase over the neat polymer is observed, while approximately 80% more cross-links are observed in the PM1-organoclay nanocomposite. Clearly, the increase in the number of cross-links would contribute to a higher modulus. Other factors could also lead to the observed behavior. To investigate this behavior further, the polymerization dynamics were examined.

Table 2. T_g and cross-link density of 3wt% organoclay in a 70:30 wt% EBGDMA:PETMP/ PEAE (PETMP:PEAE is in 1:1 molar ratio). v_e is calculated at $T_g + 50^\circ\text{C}$.

Monomer	Organoclay	T_g ($^\circ\text{C}$)	v_e (mol/m^3)
EBGDMA/PEAE/PETMP	None	22.9 ± 0.7	$5.1 \times 10^3 \pm 0.4 \times 10^3$
	Cloisite 15A	20.6 ± 0.7	$5.5 \times 10^3 \pm 0.3 \times 10^3$
	C14MA-organoclay	19.2 ± 0.4	$7.6 \times 10^3 \pm 0.3 \times 10^3$
	PM1-organoclay	21.6 ± 0.6	$9.2 \times 10^3 \pm 0.3 \times 10^3$

The polymerization behavior was further examined to better understand the thermo-mechanical properties. For clarity, the conversion profiles of the neat formulation, CL15A and PM1-organoclay systems are compared. Figure 3a shows RTIR plots of conversion versus time for the neat polymer, while Figure 3b show reaction behavior of nanocomposites containing either CL15A or PM1-organoclay systems. Methacrylate double bond conversion reaches 100% after irradiating the neat sample for 3 minutes. Both thiol and ene functional groups reach considerably less conversion in the same period (see Figure 3a). Very low ene conversion initially occurs until methacrylate double bond conversions reach approximately 60%. The ene conversion then accelerates to a final conversion of 70% after EBGDMA polymerizes to a high degree. Thiol functional groups show conversion of approximately 65% during

the same irradiation time. However, the rate of thiol conversion appears more monotonic, albeit slower than the methacrylate species. Upon incorporating organoclay into the monomer mixture, different polymerization behavior occurs. First, methacrylate double bond conversion in samples containing CL15A and PM1-organoclay reaches approximately 80% compared to the full conversion in the neat sample. Thiol functional groups reach much higher conversion levels (~80%) in the organoclay-filled formulations. However, unlike the neat formulation, addition of organoclay appears to inhibit the auto-acceleration phenomenon. Formulations that have CL15A or PM1-organoclay initially polymerize very slowly as was observed in the unfilled system. Polymerization acceleration does not occur as the polymerization proceeds, and final ene conversions of approximately 25% are reached.

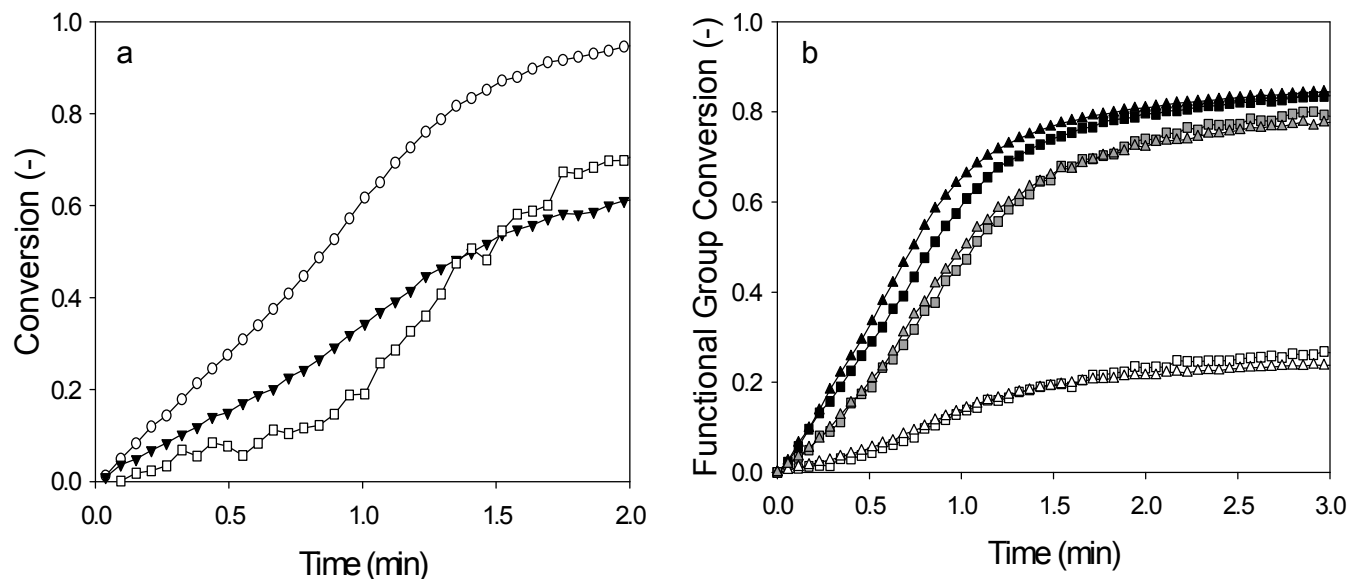


Figure 3. RTIR conversion plots of A) a 70:30wt% mixture of EBGDMA and (1:1mol functional groups) PETMP:PEAE. EBGDMA (\circ), PETMP (\blacktriangledown) and PEAE (\square). (B) Plot of a 70:30wt% mixture of EBGDMA:PETMP/PEAE (1:1mol functional groups) and 3 wt% organoclay. Acrylate (\blacksquare), ene (\square) and thiol (\blacksquare) conversions for Cloisite 15A samples and conversion of EBGDMA (\blacktriangle), PETMP (\triangle) and PEAE (Δ) in PM1-organoclay samples. Light intensity is 10 mW/cm^2 using 365 nm light.

Previous research has shown that the ene monomer does not participate actively in the reaction process in such systems during the initial stages, but becomes active after high EBGDMA conversion levels as demonstrated in Figure 3a. Thus, chain transfer to thiol occurs primarily from the EBGDMA up to the high methacrylate conversions before thiol-ene polymerization proceeds. In terms of material properties, such reaction mechanism results in more loosely cross-linked networks. It is evident that thiol-methacrylate copolymerization occurs to a significant degree in the presence of organoclay. Comparing the thiol and methacrylate functional group conversions show that chain transfer to thiol occurs to a much greater degree when organoclay is introduced into the reaction medium as shown in Figure 3b. This leads to a decrease in the amount of thiol available to copolymerize with ene monomers and may lead to the reduced conversion levels. In addition, considering that presence of organoclay could reduce polymerization rate and conversion because of light scattering and/or absorption by the particles, the overall reduction in functional group conversion is consistent with previous observations.¹⁹ The apparent high degree of chain transfer to thiol in the samples containing organoclay also influences the physical properties of the nanocomposite. Due to the weak thio-ether linkage in methacrylate-thiol

copolymers, more rubbery polymers are obtained. Indeed, this is confirmed from Table 2, in which all nanocomposites showed T_g below room temperature. The loosely cross-linked networks are more amenable to increased moduli upon incorporating organoclay into the polymer matrix as demonstrated previously.

Previous work has shown a greater impact of organoclay on the modulus of polymers as the cross-link density decreases. Because substitution of PEAE for TATATO in these thiol-ene-methacrylate systems leads to lower moduli and that organoclay could be used to modulate physical properties in more rubbery systems, the properties of ternary systems with variable cross-linker concentrations were investigated. This was accomplished by changing the amount of EBGDMA and keeping the molar ratio of PETMP/PEAE constant in the formulation. Figure 4 shows a plot of the Young's modulus (at 30°C) of the neat polymer compared to nanocomposites containing 3 wt% Cloisite 15A versus cross-linker concentration. Figure 4a shows that the Young's modulus of a PETMP/PEAE polymer increases linearly with higher loading of EBGDMA. The modulus generally increases with addition of organoclay in analogous trends as the unfilled formulations. However, the extent of modulus increase appears to be dependent on cross-linker concentration. Thus, the highest degree of increase occurs with addition of Cloisite 15A to sample with only 10 wt% EBGDMA in the thiol-ene mixture. With 10 wt% cross-linker concentration, the nanocomposite has a modulus that is approximately 40% higher than the unfilled polymer. As shown in Figure 4b, the relative change in modulus decreases somewhat monotonically up to 30 wt% EBGDMA concentration. It appears that mixtures consisting of 30 – 50 wt% methacrylate are least impacted by the organoclays as less than 10% increase in modulus occurs at those EBGDMA concentrations. However, as concentration of the cross-linker increases, the magnitude of change in the modulus generally decreases up to the 50/50 methacrylate to thiol-ene mixture.

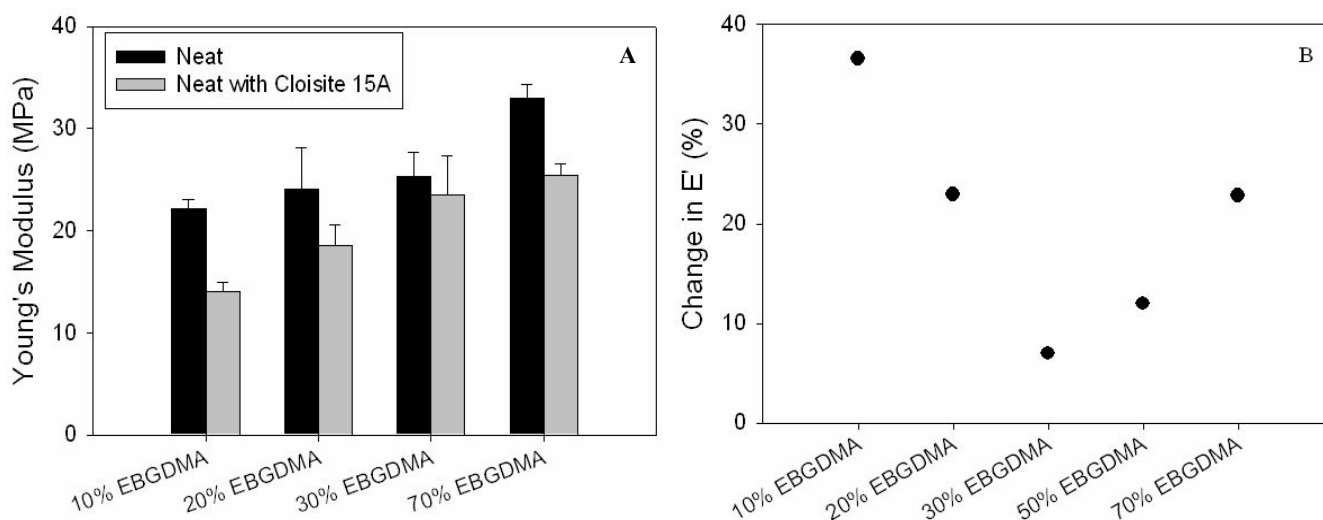


Figure 4. (A) Comparison of the Young's modulus of neat versus 3 wt% Cloisite 15A filled thiol-ene polymer with increasing EBGDMA concentration. Neat sample contain 70:30 wt% EBGDMA:PETMP/PEAE (1:1 mol PETMP:PEAE). (B) Percent change in the modulus of Cloisite 15A filled polymer relative to the unfilled polymer as a function of methacrylate concentration.

Such changes in mechanical properties of nanocomposites appear to behave similarly and are consistent with previous studies examining the correlation between polymer network structure and

added organoclay nanoparticles. Therefore, by varying the proportion of methacrylate to thiol-ene monomer in a ternary photopolymer system, it is possible to access a range of mechanical properties in a photopolymerizable nanocomposite. It should be noted also that by varying the constituent concentration, the polymerization behavior may also change as was observed earlier. To understand further how the

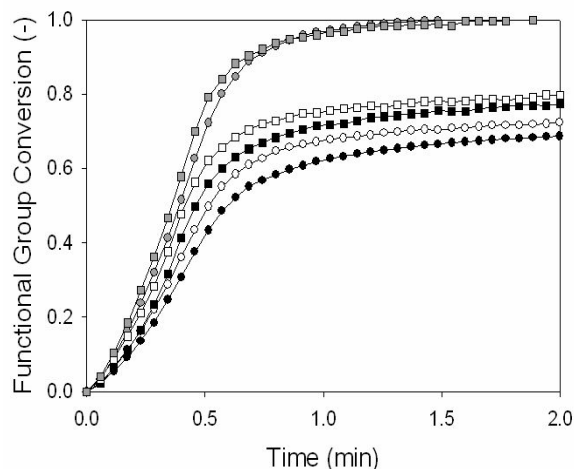


Figure 5. RTIR plot of a 10:90wt% mixture of EBGDMA:PETMP/PEAE (1:1mol functional groups) and 3 wt% organoclay. Acrylate (■), ene (□) and thiol (■) conversions for Cloisite 15A samples and conversion of EBGDMA (●), PETMP (●) and PEAE (○) in unfilled samples. Light intensity is 10 mW/cm² using 365 nm light.

photopolymerization behavior is affected by changing concentration of cross-linker in the formulation, the conversion of samples with increasing concentrations of EBGDMA and 3 wt% CL15A was examined via RTIR. Figures 5 show the functional group conversion versus time plot for samples with 10 wt% EBGDMA. With only 10 wt% methacrylate in the formulation, the polymerization behavior differs significantly from the formulation containing 70 wt% EBGDMA discussed previously. Full conversion of thiol functional groups is obtained in the neat sample. Both ene and methacrylate conversion occurs at the same rate and ultimately to the same level. Approximately 70% PEAE and EBGDMA conversion are observed respectively. In addition, while ene conversion is delayed until high methacrylate double bond conversion in the samples containing 70 wt% EBGDMA, no significant difference in the rate of both methacrylate and ene conversions are observed here. Addition of CL15A to the formulation does not alter the photopolymerization profile. With 3 wt% CL15A in the formulation, 100% thiol conversion is observed. Methacrylate and ene double bond conversions are higher (ca. 80%) with CL15A.

Conclusion

Addition of thiol monomers to (meth)acrylate systems has been explored to expanding the breadth of physical properties achievable in traditional free radical photopolymers. Herein, the influence of added organoclay on the modulus and glass transition temperatures of ternary polymer systems comprising methacrylate, allyl ether and thiol monomers have been investigated. In binary PETMP/TATATO polymers, addition of non-polymerizable organoclays reduces the Young's modulus of the polymer. In the more rubbery PETMP/PEAE formulation, addition of the methacrylate species increases the Young's modulus slightly. Incorporating an ethoxylated bisGMA monomer into this thiol-ene mixture increases the Young's modulus compared to neat thiol-ene photopolymer. Here, significant increases are observed with addition of polymerizable organoclay. T_g remains relatively unchanged after adding organoclay. The degree to which Young's modulus is altered upon adding organoclay depends on cross-linker concentration. At low EBGDMA concentrations, addition of organoclay leads to much greater increases in E' . The magnitude of increase decreases as cross-linker concentration is raised to 50% at which the lowest percentage change occurs. Finally, changing cross-linker concentration changes the polymerization behavior with either thiol or methacrylate species reacting at the fastest rate and highest conversion when in the highest concentrations. Thus, at low EBGDMA concentration, thiol monomers polymerize faster and to higher conversion levels relative to the ene or methacrylate monomers. Similarly, at 70% EBGDMA concentration, methacrylate double bonds convert to a higher

degree at a faster rate with the ene species exhibiting intermediate polymerization and conversion levels. Adding polymerizable organoclay to these formulations induces similar ene and methacrylate conversion rates and levels. These studies demonstrate another route by which photopolymer properties can be modulated with addition of polymerizable organoclays.

Acknowledgements

The authors gratefully acknowledge financial support from the National Science Foundation (CTS-0626395) and the I/UCRC Center for Fundamentals and Applications of Photopolymerization.

References

1. Marvel, C. S.; Chambers, R. R. *J. Am. Chem. Soc.* **1948**, 70, 993.
2. Hoyle, C. E.; Lee, T. Y.; Roper, T. *J. Polym. Sci. A: Polym. Chem.*, **2004**, 42, 5301.
3. Koval', I. V. *Russ. J. Org. Chem.* **2007**, 43, 327.
4. Cramer, N. B.; Reddy, S. K.; Cole, M.; Hoyle, C.; Bowman, C. N. *J. Polym. Sci.: Polym. Chem.* **2004**, 42, 5817.
5. Giannelis, E. P. *Adv. Mater.* **1996**, 8, 29.
6. Usuku, A.; Kojima, Y.; Kawasumi, M.; Okada, A.; Fukushima, Y.; Kurauchi, T., Kamigaito, O. *J. Mater. Res.* **1993**, 8, 1185.
7. Lee, T. Y.; Bowman, C. N. *Polymer*, **2006**, 47, 6057.
8. Sangermano, M.; Gross, S.; Priola, A.; Rizza, G.; Sada, C. *Macromol. Chem. Phys.* **2007**, 208, 2560.
9. Heliotis, G.; Stavrinou, P. N.; Bradley, D. D. C.; Gu, E.; Griffin, C.; Jeon, C. W.; Dawson, M. D. *Appl. Phys. Lett.* **2005**, 87, 103505/1.
10. Caseri, W. *Macromol. Rapid Comm.* **2000**, 21, 705.
11. Yurasova, I. V.; Antipov, O. L.; Ermolaev, N. L.; Cherkasov, V. K.; Lopatina, T. I.; Chesnokov, S. A.; Ilyina, I. G. *Phys. Sol. State* **2005**, 47, 129.
12. Nikonorova, N. A.; Barmatov, E. B.; Pebalk, D. A.; Barmatova, M. V.; Dominguez-Espinosa, G.; Diaz-Calleja, R.; Pissis, P. *J. Phys. Chem. C* **2007**, 111, 8451.
13. Murugaraj, P.; Mainwaring, D. E.; Jakubov, T.; Mora-Huertas, N. E.; Khelil, N. A.; Siegele, R. *Sol. State Comm.* **2006**, 137, 422.
14. Aguzzi, C.; Cerezo, P.; Viseras, C.; Caramella, C. *Appl. Clay Sci.* **2007**, 36, 22.
15. LeBaron, P. C.; Wang, Z.; Pinnavaia, T. J. *Appl. Clay Sci.* **1999**, 15, 11.
16. Uhl, F. M.; Davuluri, S. P.; Wong, S. C.; Webster, D. C. *Chem. Mater.* **2004**, 16, 1135.
17. Owusu-Adom, K.; Guymon, C. A. unpublished data
18. Owusu-Adom, K.; Guymon, C. A. *Macromolecules* **2008**.
19. Owusu-Adom, K.; Guymon, C. A. *Polymer* **2008**, 49, 2636.
20. Carioscia, J. A.; Stansbury, J. W.; Bowman, C. N. *Polymer* **2007**, 48, 1526.
21. Katti, K. S.; Sikdar, D.; Katti, D. R.; Ghosh, P.; Verma, D. *Polymer* **2006**, 47, 403.
22. Lee, T. Y.; Smith, Z.; Reddy, S. K.; Cramer, N. B.; Bowman, C. N. *Macromolecules* **2007**, 40, 1466.
23. Lee, T. Y.; Carioscia, J.; Smith, Z.; Bowman, C. N. *Macromolecules* **2007**, 40, 1473.
24. Lecamp, L.; Houllier, F.; Youssef, B.; Bunel, C. *Polymer* **2001**, 42, 2727.